White Rose Research Online

eprints@whiterose.ac.uk
https://eprints.whiterose.ac.uk
Universities of Leeds, Sheffield and York

Deposited via The University of Sheffield.

White Rose Research Online URL for this paper:
https://eprints.whiterose.ac.uk/id/eprint/188905/

Version: Accepted Version

Article:
Liu, Z.-H., Nie, J., Wei, H.-L. et al. (2022) Second-order ESO-based current sensor fault-tolerant strategy for sensorless control of PMSM with B-phase current. IEEE/ASME Transactions on Mechatronics, 27 (6). pp. 5427-5438. ISSN: 1083-4435

https://doi.org/10.1109/tmech.2022.3182134

© 2022 IEEE. Personal use of this material is permitted. Permission from IEEE must be obtained for all other users, including reprinting/ republishing this material for advertising or promotional purposes, creating new collective works for resale or redistribution to servers or lists, or reuse of any copyrighted components of this work in other works. Reproduced in accordance with the publisher's self-archiving policy.

Reuse
Items deposited in White Rose Research Online are protected by copyright, with all rights reserved unless indicated otherwise. They may be downloaded and/or printed for private study, or other acts as permitted by national copyright laws. The publisher or other rights holders may allow further reproduction and re-use of the full text version. This is indicated by the licence information on the White Rose Research Online record for the item.

Takedown
If you consider content in White Rose Research Online to be in breach of UK law, please notify us by emailing eprints@whiterose.ac.uk including the URL of the record and the reason for the withdrawal request.

UNIVERSITY OF LEEDS
University of Sheffield
UNIVERSITY of York

Final Manuscript Accepted for publication by IEEE/ASME Transactions on Mechatronics, June 2022

ESO Based Current Estimation for PMSM Sensorless control with B-Phase Current Sensor

Zhao-Hua Liu, *Senior Member*, IEEE, Jie Nie, Hua-Liang Wei, Lei Chen, Fa-Ming Wu, and Ming-Yang Lv

***Abstract*— Usually, two phase current sensors are required to realize sensorless control of permanent magnet synchronous motor (PMSM). However, once the phase current sensor fails, the whole system will not work. In this paper, a novel second order extended state observer (SO-ESO) based current estimation method for realizing PMSM sensorless control and multi-parameter identification using only B-phase current sensor is proposed, which can significantly reduce the system cost and improve the reliability. In order to reduce the chattering of the system, a sigmoid function is introduced in the SO-ESO. In addition, a SO-ESO based parallel speed and multi-parameter identification scheme are proposed by using two model reference adaptive system observer (MRASO). The first MRASO is designed based on super twisting algorithm (STA-MRASO) with a corrective feedback loop and is used for estimating rotor speed and position. The second MRASO only needs to identify inductance and permanent flux because the stator resistance is estimated by SO-ESO. The second MRASO and SO-ESO updates the three identified electrical parameters and estimation currents to the first MRASO to achieve high robustness sensorless control. The relevant results show that the scheme gives good results, and the system has good dynamic performance and strong robustness.**

***Index Terms*—Model reference adaptive system, extended state observer (ESO), PMSM, sensorless control, parameter estimation, fault tolerant control.**

I. Introduction[1]

In recent years, permanent magnet synchronous motor (PMSM) have been widely used in industrial production, national defense and daily life. Compared with induction motor and DC motor, PMSM has the advantages of high efficiency, high torque current ratio, compact structure, simple mechanical structure and easy maintenance [1], [2]. However, in many applications, such as computer numerical control machine tools, robots, and electric vehicles, the requirement for control performance of PMSM becomes higher [3], [4]. At the same time, it is required that the drive system be simple, safe and reliable. In doing so, two major issues need to be addressed: stable acquisition of current signal and sensorless control.

Generally, one position sensor and two phase current sensors (without neutral line) are indispensable to the typical permanent magnet synchronous motor (PMSM) drive to ensure the normal operation of feedback control [5]. However, the control performance of drive system can be deteriorated and even fail to work normally once the phase current sensor fails. Therefore, the introduction of multiple physical sensors may reduce the security and stability of the system [6]. When the rotor speed of PMSM tends to zero or very low, it is difficult to control the motor speed accurately without position sensor. At the same time, if the output characteristics of multiple phase current sensors do not match, the control performance of the system can be significantly degraded, such as the nonzero offset and the gain drift, which can cause torque ripple. Consequently, in order to make the PMSM drive system more efficient, economical and safer, reducing the current sensor has become an attractive option in recent years.

One of the key solutions to ensure the stable acquisition of current signals is to use fault-tolerant control with current sensors. Fault-tolerant control methods for current sensors can be roughly classified into two groups [7]: active control and passive control. The former responses to a system failure (e.g. caused by a current sensor fault) actively by switching the system to another control mode (e.g. from the closed-loop vector control dependent on the sensor to the open-loop control independent of the sensor) to maintain the desired performance. The latter is to reconstruct the current signal from the observer instead of the incorrect feedback signal, so as to continue the closed-loop vector control [8]; in the latter method, controllers are usually designed to be robust enough to ensure the system not to be too vulnerable or sensitive to known system component failures. The first method is simple, but the performance of open-loop control is worse than that of closed-loop vector control, which reduces the control performance of the system to a great extent. In contract, the second method does not need to change the structure of the closed-loop system, so as to control the driving system with high performance. However, the performance of closed-loop vector control depends on the quality of the designed current observer after the fault occurs. An open question relating to current sensor fault-tolerant control is: how to design a high-quality current observer?

Broadly two types of methods have been reported in the literature for fault-tolerant current estimation. The first type uses DC bus current method [9], [10]. Although such methods are usually effective, their disadvantages are obvious: the DC bus current is unmeasurable under the condition of low speed PMSM range, because the duration of the active switching state very short. At the same time, there are some regions that cannot be measured in the output voltage hexagon. Therefore, it is difficult to sample the DC bus current. In order to solve these problems and obtain high-accuracy reconstruction current, a variety of advanced DC-link current reconstruction schemes based on PWM technology are offered [11], [12]. Although the precision of current estimation is increased with these methods, the associated implementation algorithms

[1] Z.-H. Liu ,J. Nie, L. Chen and M.-Y Lv are with the School of Information and Electrical Engineering, Hunan University of Science and Technology, Xiangtan 411201, China (e-mail: zhaohualiu2009@hotmail.com; jienie@mail.hnust.edu.cn; chenlei@hnust.edu.cn; 1040133@hnust.edu.cn).
H.-L. Wei is with the Department of Automatic Control and Systems Engineering, University of Sheffield, Sheffield S1 3JD, U.K. (e-mail: w.hualiang@sheffield.ac.uk).
F.-M. Wu is with the Department of Wind Power Business Division, CRRC Zhuzhou Institute, Zhuzhou, .412000, China. (e-mail: wufm@csrzic.com).

are complicated. In [13], Xu et. al proposed a field-oriented-control (FOC) strategy of PMSM drives using single phase current. This method proposed a new strategy of 3-phase current reconstruction using zero voltage vector sampling, in which only an isolated current sensor is needed and DC bus current sensor is needless. Unfortunately, the performance of current control will be affected because a single current sensor is sampled twice in each PWM period. The second type is using adaptive observer-based method but their limitation is to assume that the stator resistance changes slowly [14].

On the other hand, the use of encoders, resolvers, Hall effect sensors or other mechanical position sensors can increase the maintenance costs and decrease the system robustness [15]-[17]. So naturally, the sensorless control strategy have attracted extensive attention in the past few decades. Depending on the speed range of PMSM operation, position sensorless control methods can be divided into two categories, namely, saliency-based high-frequency (HF) signal injection method and model-based back EMF method. Although the HF method is suitable for sensorless control of PMSM at low or zero speed range, this method may lead to torque ripple and additional loss, which has a negative effect on the dynamic performance and operation quality of the system [18]. On the contrary, the EMF method has been extensively investigated because it does not require the injection of additional signals. It is widely recognized that the model-based method is appropriate for PMSM to work at medium and high speeds. In [19], an extended Luenberger observer was proposed which provides a promising scheme because of robust to parameter variations. The main disadvantage of the method is that it is hard to implement due to its complexity. Several intelligent schemes, such as fuzzy logic and neural networks have been proposed for estimation rotor speed [20], [21]. However, these intelligent method usually need large amount of calculation. Another powerful method is model reference adaptive system (MRAS) [22]-[25], which has the advantages of simplicity, good stability and small amount of calculation. MRAS has been testified to be one of the best methods introduced in the literature. An adaptive PI regulator is commonly used in the traditional MRAS and it cannot meet high performance control. Therefore, a variety of solutions with more advanced algorithms are proposed, which provide alternatives to the adaptation mechanism for MRAS scheme. In [22], a fuzzy logic controller was employed in MRAS for speed regulation so that the system becomes more robust than a PI controller to deal with parameter uncertainties and sensor noises. In [23], an artificial neural network method was utilized in MRAS scheme for stator resistance estimation and good experimental results have been obtained. However, the above schemes do not solve the adverse impact of parameter changes on MRAS from the root. In addition, these schemes need large amount of calculation, which is not conducive to engineering practice. The steady-state module of PMSM is often utilized as a reference; consequently, robustness may be difficult to achieve if there is a parameter mismatch or load with a sudden change during the working operation under the low speed range [26], [27]. Therefore, in order to achieve high-performance sensorless control, it is necessary to combine multi-parameter identification.

In practical control systems, many factors such as load, temperature, and device age can impact the estimation of the electrical parameters of PMSMs including stator resistance, inductance, and permanent magnet flux linkage. However, for most speed / position sensorless control algorithms, these parameters are needed for estimating the rotor's position; changes in these parameters can cause errors in the position estimation [28]. As a result, any changes to these parameters may have an impact on the actual system's control performance. Combining on-line parameter identification technology with PMSM speed sensorless control can greatly improve the robustness and accuracy of the control system. Consequently, a variety of multi-parameter identification techniques such as extended Kalman filter (EKF) [29], [30], recursive least squares (RLS) [31], [32], and MRAS schemes [33]-[36] have been proposed. In [30], the EKF scheme gave appropriate experimental result in parameter identification. Nevertheless, the control algorithm has some limitations such as complex algorithmic structure, requirement of proper initialization. The RLS scheme for estimating electrical parameters proposed in [31] and [32] has a fast convergence speed. However, due to the algorithm involves a large number of differential equations, the performance of microprocessor decreases and the system response is slow. In [33] and [34], a MRAS observer (MRASO) was introduced for estimating stator resistance and flux. Although this method has the advantages of small amount of calculation, fast response speed and high accuracy of identification results, the inductance cannot be estimated due to the lack of rank. Therefore, once the inductance changes, it is bound to have an impact on the vector control of PMSM at low speed.

Traditionally, the key of Field-oriented-control (FOC) strategy can obtain a precise 3-phase current through two current sensors to calculate the excitation current i_d and torque current i_q. Furthermore, encoders, resolvers or other mechanical sensors are indispensable for measuring position and speed. However, the introduction of multiple physical sensors may reduce the security and stability of the system, and increases the cost and complexity of maintenance. Therefore, in order to reduce the number of physical sensors, it is necessary to estimate the stator current and achieve sensorless control with robustness to parameter variation. In this paper, a scheme where *d*-axis inductance is made equal to *q*-axis inductance in surface mounted PMSM is employed. There are three electrical parameters need to be estimated: i.e., stator resistance, inductance and permanent flux. The main contributions of this paper are as follows:

1) Different from the traditional 3-phase current reconstruction strategy, a novel second order extended state observer (SO-ESO) scheme is proposed for estimating the *d-q* axis stator current and time varying resistance without knowing the precise model information. When a fault occurs in the A-C 2-phase current sensor, the proposed scheme uses only a B-phase current sensor to estimate the information of the *d-q* axis stator current, achieving a high-performance sensorless control function. Furthermore, in order to increase the dynamic performance and decrease the chattering problem, a sigmoid function is introduced to replace the traditional sign function in the SO-ESO. As can be seen

in Sections II and III, the principle of this scheme is easy to implement.

2) A SO-ESO based parallel speed and multi-parameter identification scheme is proposed, for the first time, by using two MRASO. The first MRASO only needs to identify inductance and permanent flux because the stator resistance is estimated by SO-ESO. The second MRASO, based on a super twisting algorithm (STA-MRASO), is designed to realize sensorless control. Furthermore, a corrective feedback loop is added by which the convergence speed of the difference between the outputs of the reference model and the adjustable model is accelerated. The second MRASO and SO-ESO updates the three identified electrical parameters and estimated *d-q* axis stator current to the STA-MRASO for achieving high robustness sensorless control. To the best of our knowledge, no result on such observers have been reported in the literature.

In summary, this control system can simultaneous estimate the following seven parameters: 2-phase *d-q* axis stator current, rotor speed, rotor position, time varying stator resistance, inductance and permanent flux.

The paper is organized as follows. In Section II-A, we first propose the mathematical model of surface mounted PMSM. In Section II-B, the current estimation scheme based ESO is introduced. In Section III, we introduce two MRAS observer for realizing sensorless control and parameter identification. The relevant results and detailed analysis are given in Section IV. Finally, a concise conclusion is provided in Section V.

II. PMSM Drive System Based on Current Estimation

A. Modeling of SPMSM

As we know, the 3-phase surface-mounted PMSM has the characteristics of $L_d=L_q=L_\alpha=L_\beta=L$ and the mathematical model can be expressed as:

$$\begin{cases} \dfrac{di_d}{dt}=\dfrac{1}{L}\left(u_d-R_s i_d+\mathrm{p}\omega_r L i_q\right) \\ \dfrac{di_q}{dt}=\dfrac{1}{L}\left(u_q-R_s i_q-\mathrm{p}\omega_r\left(L i_d+\psi_m\right)\right) \end{cases} \tag{1}$$

$$\begin{cases} \dfrac{di_\alpha}{dt}=\dfrac{1}{L}\left(u_\alpha-R_s i_\alpha+\mathrm{p}\omega_r\psi_m\sin\theta_e\right) \\ \dfrac{di_\beta}{dt}=\dfrac{1}{L}\left(u_\beta-R_s i_\beta-\mathrm{p}\omega_r\psi_m\cos\theta_e\right) \end{cases} \tag{2}$$

where p is the number of pole pairs. The subscripts d and q represent the d and q axis, respectively. u_d and u_q are stator voltage components, i_d and i_q are stator current components, L_d and L_q are the stator inductances, R_s is the stator resistance, ω_r is the mechanical angular velocity, ψ_m is the permanent magnet flux, and θ_e is the rotor electrical positions. Note that the change of the mechanical angular velocity, ω_r, can be formulated as:

$$J\frac{d\omega_r}{dt}=T_e-T_l-B\omega_r-T_f \tag{3}$$

$$T_e=\frac{3}{2}\mathrm{p}\psi_m i_q \tag{4}$$

where J and B are inertia and viscous friction, respectively. T_l and T_f are load torque and coulomb friction torques, respectively. T_e is the electrical torque.

B. Design of SO-ESO Using B-Phase Current Sensor

The purpose of designing second order extended state observer (SO-ESO) is to make the PMSM drive system high-performance work for reducing current sensors. The SO-ESO

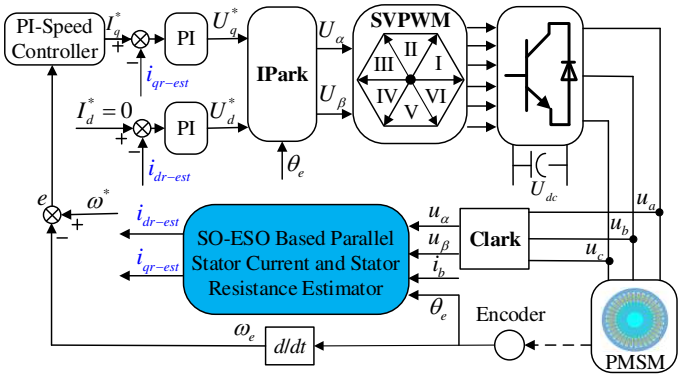

Fig. 1. The block diagram of FOC PMSM drive system using SO-ESO scheme with B-phase current sensor.

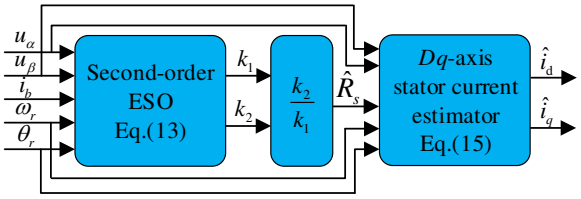

Fig. 2. *d-q* axis currents and stator resistance estimator using SO-ESO.

based vector control system is shown in Fig. 1.

The designed SO-ESO is to identify the *d-q* axis stator current and stator resistance varying with temperature while B-phase current sensor is working. In the implementation of SO-ESO scheme, three assumptions are considered:

1)Only B-phase current sensor is working and the other 2-phase current sensors are in fault state.

2)In practical applications, the stator resistance R_s varies with temperature, so R_s is considered as a variable.

3) There is no saturation in the magnetic circuit.

$$\begin{bmatrix} i_a \\ i_b \\ i_c \end{bmatrix}=\begin{bmatrix} 1 & 0 \\ -1/2 & \sqrt{3}/2 \\ -1/2 & -\sqrt{3}/2 \end{bmatrix}\begin{bmatrix} i_\alpha \\ i_\beta \end{bmatrix} \tag{5}$$

where i_a, i_b, and i_c are 3-phase stator currents in *abc* coordinate system. Based on (5), i_b can be reported as

$$2i_b=-i_\alpha+\sqrt{3}i_\beta \tag{6}$$

Using (2), equation (6) can be further written as:

$$\frac{di_b}{dt}=\frac{\sqrt{3}}{2L}\left[u_\beta-R_s\left(\frac{1}{\sqrt{3}}i_\alpha+\frac{2}{\sqrt{3}}i_b\right)-\mathrm{p}\omega_r\psi_\mathrm{m}\cos\theta_e\right]-$$
$$\frac{1}{2L}\left(u_\alpha-R_s i_\alpha+\mathrm{p}\omega_r\psi_\mathrm{m}\sin\theta_e\right) \tag{7}$$
$$=\frac{\sqrt{3}u_\beta-u_\alpha-2R_s i_b-\mathrm{p}\omega_r\psi_\mathrm{m}\left(\sqrt{3}\cos\theta_e+\sin\theta_e\right)}{2L}$$

Assume $x_1=i_b$ and define

$$u=\frac{1}{2L}\left[u_\alpha \;\; u_\beta \;\; \psi_m\omega_e\sin\theta_e \;\; \psi_m\omega_e\cos\theta_e\right]^{\mathrm{T}}$$
$$D=\left[-1 \;\; \sqrt{3} \;\; -1 \;\; -\sqrt{3}\right] \tag{8}$$

where $\omega_e=\mathrm{p}\omega_r$ is the electric angle speed.

Then the extended state space equation can be deduced

$$\begin{cases}\dot{x}_1=-\dfrac{R_s x_1}{L}+Du\\ y_0=x_1\end{cases} \tag{9}$$

where u is the input, y_0 is the output, and D is the input matrix.

Furthermore, the term $R_s x_1$ in (9) can be regarded as an unknown quantity due to R_s varies with temperature. Therefore, $R_s x_1$ could be extended to a new state

$$x_2=R_s x_1 \tag{10}$$

Let $h(t)=\dot{x}_2$, then

$$h(t)=\dot{R}_s x_1+R_s\dot{x}_1=\dot{R}_s i_b+R_s\dot{i}_b \tag{11}$$

In addition, equation (9) can be depicted as

$$\begin{cases}\dot{x}_1=-x_2/L+Du\\ \dot{x}_2=h(t)\\ y_0=x_1\end{cases} \tag{12}$$

It can be known that the state-space system (12) is observable. By introducing a sigmoid function, the associated SO-ESO can be obtained

$$\begin{cases}\zeta=k_1-x_1\\ \dot{k}_1=-k_2/L+Du_1-w_1\zeta\\ \dot{k}_2=-w_2 sigmoid\ (\zeta,\tau,\delta)\end{cases} \tag{13}$$

where ζ is the error, w_1 and w_2 are the positive gains of observer, $k_1=\hat{x}_1$ and $k_2=\hat{x}_2=\hat{x}_1\hat{R}_s$ ($\hat{x}_1$ and $\hat{x}_2$ are the estimated values of x_1 and x_2, respectively). τ is a positive number, and $sigmoid\ (\zeta,\tau,\delta)$ is an exponential function:

$$sigmoid(\zeta,\tau,\delta)=\begin{cases}|\zeta|^{\tau}\ sign(\zeta) & |\zeta|>\delta\\ \dfrac{\zeta}{\delta^{1-\tau}} & |\zeta|<\delta\end{cases} \tag{14}$$

The estimation value of R_s is $\hat{R}_s=k_2/k_1$. Therefore, the observer of *d-q* axis currents in (1) can be rewritten as

$$\begin{cases}\dfrac{d\hat{i}_d}{dt}=\dfrac{1}{L}\left(u_d-\hat{R}_s\hat{i}_d+\mathrm{p}\omega_r L\hat{i}_q\right)\\ \dfrac{d\hat{i}_q}{dt}=\dfrac{1}{L}\left(u_q-\hat{R}_s\hat{i}_q-\mathrm{p}\omega_r\left(L\hat{i}_d+\psi_m\right)\right)\end{cases} \tag{15}$$

According to [15], if the following inequality holds

$$0.25w_1^2>w_2>h_0 \tag{16}$$

The proposed SO-ESO is stable and can guarantee that k_1 and k_2 quickly converges to x_1 and x_2. Therefore, $\hat{R}_s$ converges to the real value R_s. By combining (13)-(15), the diagram of the proposed SO-ESO can be depicted using Fig. 2. It needs the information of the stator voltage, rotor speed and position for estimating the *d-q* axis current and resistance when only B-phase current sensor is available.

For the proposed SO-ESO, there are three points to note:

1) From Fig. 2, it can be known that the accuracy of the measured B-phase current will affect the quality of ESO (12).

2) The principles of parameter setting of (13) are generally as follows: i) $0<\tau\le 1$. ii) δ represents the interval width near the origin; it relates to system steady state error. The selection range of δ is [0.0001, 1]. If δ is too small, it may cause high frequency pulsation to the system. On the contrary, if δ is too large, the effect of nonlinear feedback control can not be achieved. In the practical engineering, it is often selected as 0.01. iii) The value of w_j (j=1, 2) should be combined with the tracking performance of the system. If w_1 is large enough, it will reduce the tracking time but may suffer system oscillation or overshoot. Generally speaking, the value of w_1 is 20~100 times of w_2. There is a compromise between w_j (j=1, 2) and δ for obtaining better performance.

3) The *d-q* axis currents estimated by SO-ESO is used in the vector control system of PMSM (shown in Fig. 1).

III. Parameter Estimation Based Sensorless Control

A. Design of STA-MRASO with Error Correction Link

The core mission of the control system is to estimate the rotor speed and rotor position accurately even there is a big change of working condition. For this purpose, the MRASO is employed for calculating the rotor speed and position. An adaptive PI regulator is commonly used in the MRASO [23].

$$\frac{d}{dt}\begin{bmatrix}\tilde{i_d}\\ \tilde{i_q}\end{bmatrix}=\begin{bmatrix}-R/L & \omega_{\mathrm{r}}\\ -\omega_{\mathrm{r}} & -R/L\end{bmatrix}\begin{bmatrix}\tilde{i_d}\\ \tilde{i_q}\end{bmatrix}+\frac{1}{L}\begin{bmatrix}\tilde{u_d}\\ \tilde{u_q}\end{bmatrix} \tag{17}$$

$$U_s^{\sim}=\begin{bmatrix}\tilde{u_d}\\ \tilde{u_q}\end{bmatrix},I_{\mathrm{s}}^{\sim}=\begin{bmatrix}\tilde{i_d}\\ \tilde{i_q}\end{bmatrix},I_s=\begin{bmatrix}\tilde{\hat{i}_d}\\ \tilde{\hat{i}_q}\end{bmatrix} \tag{18}$$

$$\begin{cases}\tilde{i_d}=i_d+\dfrac{\psi_m}{L}, \quad \tilde{i_q}=i_q\\ \tilde{u_d}=u_d+R\dfrac{\psi_m}{L},\ \tilde{u_q}=u_q\end{cases} \tag{19}$$

where $U_s^{\sim}$ is a stator voltage vector, and $I_s^{\sim}$ is a stator current vector. The adjustable model of MRAS can be obtained by replacing the estimated values of current and speed in (17)

$$\frac{d}{dt}\begin{bmatrix}\tilde{\hat{i}_d}\\ \tilde{\hat{i}_q}\end{bmatrix}=\begin{bmatrix}-R/L & \hat{\omega}_{\mathrm{r}}\\ -\hat{\omega}_{\mathrm{r}} & -R/L\end{bmatrix}\begin{bmatrix}\tilde{\hat{i}_d}\\ \tilde{\hat{i}_q}\end{bmatrix}+\frac{1}{L}\begin{bmatrix}\tilde{u_d}\\ \tilde{u_q}\end{bmatrix} \tag{20}$$

As can be seen from Fig. 3, the output of the reference model is the actual value of stator current, which can be directly obtained by SO-ESO. The output of the adjustable model is the estimated value of stator current. By comparing (17) and (20), the error dynamic equation can be deduced as

$$\begin{bmatrix}\dot{e}_d\\ \dot{e}_q\end{bmatrix}=\mathbf{A}\begin{bmatrix}e_d\\ e_q\end{bmatrix}-\mathbf{J}\left(\omega_{\mathrm{r}}-\hat{\omega}_{\mathrm{r}}\right)\begin{bmatrix}\tilde{\hat{i}_d}\\ \tilde{\hat{i}_q}\end{bmatrix} \tag{21}$$

$$e_d=\tilde{i_d}-\tilde{\hat{i}_d},e_q=\tilde{i_q}-\tilde{\hat{i}_q},\mathbf{A}=\begin{bmatrix}-R/L & \omega_{\mathrm{r}}\\ -\omega_{\mathrm{r}} & -R/L\end{bmatrix},\mathbf{J}=\begin{bmatrix}0 & -1\\ 1 & 0\end{bmatrix}$$

where e_d and e_q are the estimation errors corresponding to excitation current and torque current, respectively. From Popov hyperstability theory, the estimated speed is

$$\hat{\omega}_{\mathrm{r}}=\left(K_p+\frac{K_{\mathrm{i}}}{s}\right)\left(i_d\hat{i}_q-\hat{i}_d i_q-\frac{\psi_m}{L}\left(i_q-\hat{i}_q\right)\right) \tag{22}$$

where K_p and K_i are proportional coefficient and integral coefficient, respectively; $1/s$ is integral operator.

When the error between the reference model output and the adjustable model output converges to zero, the estimated value of rotor speed will reach the corresponding actual value. From (22) it can be seen that the estimated speed is an adjustable parameter in the adjustable model.

In order to further improve the convergence speed of the error between the outputs of the two models in the traditional MRASO, this paper improves the MRASO structure by introducing an error correction term, so that the output of the adjustable model is continuously corrected by feedback and improve the convergence speed of the error between the outputs of the two models. Similarly, an adjustable model is constructed based on (17) containing speed information. Now re-write equation (17) as

$$\dot{\mathbf{i}}_s = \mathbf{A}\mathbf{i}_s + \mathbf{B}\mathbf{u}_\mathbf{s} + \mathbf{d} \tag{23}$$

$$\mathbf{i}_s = \begin{bmatrix} i_d \\ i_q \end{bmatrix}, \mathbf{u}_s = \begin{bmatrix} u_d \\ u_q \end{bmatrix}, \mathbf{B} = \begin{bmatrix} 1/L & 0 \\ 0 & 1/L \end{bmatrix}, \mathbf{d} = \begin{bmatrix} 0 \\ -\psi_m \omega_\mathrm{r} / L \end{bmatrix} \tag{24}$$

Then, replace the variable in (23) by the estimated value and add the error correction to the equation, then the adjustable model in the form of state observer is

$$\frac{d\hat{\mathbf{i}}_\mathrm{s}}{dt} = \mathbf{A}\hat{\mathbf{i}}_\mathrm{s} + \mathbf{B}\mathbf{u}_\mathrm{s} + \mathbf{d} + \mathbf{K}\left(\hat{\mathbf{i}}_\mathrm{s} - \mathbf{i}_\mathrm{s}\right) \tag{25}$$

$$\hat{\mathbf{i}}_s = \begin{bmatrix} \hat{i}_d \\ \hat{i}_q \end{bmatrix}, \mathbf{A} = \begin{bmatrix} -R/L & \hat{\omega}_\mathrm{r} \\ -\hat{\omega}_\mathrm{r} & -R/L \end{bmatrix}, \mathbf{d} = \begin{bmatrix} 0 \\ -\psi_m \hat{\omega}_\mathrm{r} / L \end{bmatrix} \tag{26}$$

where $\mathbf{K}\left(\hat{\mathbf{i}}_\mathrm{s} - \mathbf{i}_\mathrm{s}\right)$ is the added error correction term $\mathbf{K}$ is the feedback correction gain matrix, and the selection of $\mathbf{K}$ should meet the stability requirements of the observer. Arraignment (23) and (25), yields

$$\begin{bmatrix} \dot{e}_d \\ \dot{e}_q \end{bmatrix} = (\mathbf{A}+\mathbf{K}) \begin{bmatrix} e_d \\ e_q \end{bmatrix} - \mathbf{J}\left(\omega_\mathrm{r} - \hat{\omega}_\mathrm{r}\right) \begin{bmatrix} \hat{i}_d \\ \hat{i}_q \end{bmatrix} - \frac{\psi_m}{L} \begin{bmatrix} 0 \\ \omega_\mathrm{r} - \hat{\omega}_\mathrm{r} \end{bmatrix} \tag{27}$$

where $e_d = i_d - \hat{i}_d$, $e_q = i_q - \hat{i}_q$, and $\mathbf{J} = \begin{bmatrix} 0 & -1 \\ 1 & 0 \end{bmatrix}$.

Similarly, the actual value of the stator current can be obtained by coordinate transformation of the measured 3-phase current. According to Popov's hyperstability theory, in order to meet the stability requirements of the observer and combined with the principle of pole assignment, the feedback correction gain matrix $\mathbf{K}$ can be selected as

$$\mathbf{K} = \begin{bmatrix} -g_1 & g_2 \\ -g_2 & -g_1 \end{bmatrix}, \begin{cases} g_1 = (k-1)\dfrac{R}{L}, & k \geq 1 \\ g_2 = (k-1)\hat{\omega}_\mathrm{r} \end{cases} \tag{28}$$

where k is a constant greater than 1, which can be obtained

$$\mathbf{A}+\mathbf{K} = \begin{bmatrix} -k\dfrac{R}{L} & k\omega_\mathrm{r} \\ -k\omega_\mathrm{r} & -k\dfrac{R}{L} \end{bmatrix} \tag{29}$$

It can be seen from (29) that the diagonal elements of the matrix are negative, meeting the stability requirements. Further, comparing the matrices $\mathbf{A}$ and ($\mathbf{A}$+$\mathbf{K}$) in (23) and (29), the adaptive observer used in this paper forms a closed-loop state estimation due to the addition of feedback correction term compared with the traditional MRASO, so it speeds up the convergence speed of the error between the output of the reference model and the output of the adjustable model. In order to avoid introducing excessive modeling error and affecting the smooth operation of the system, the selection of k should not be too large.

The adaptive mechanism represented by (22) can be regarded as a PI controller. Then, in order to improve the robustness of the observer and alleviate the chattering problem of traditional sliding mode, a super twisting algorithm (STA) is introduced to replace the PI adaptive mechanism. STA is a second-order sliding mode algorithm. Owing to its structural characteristics, STA has good robustness and can alleviate the chattering problem of traditional sliding mode to a certain extent. Its basic form is

$$\begin{cases} \dot{x}_1 = -k_1 \left|x_1\right|^{\frac{1}{2}} \operatorname{sign}\left(x_1\right) + x_2 \\ \dot{x}_2 = -k_2 \operatorname{sign}\left(x_1\right) \end{cases} \tag{30}$$

where x_1 and x_2 are state variables; $\dot{x}_1$ and $\dot{x}_2$ are derivatives of corresponding variables; k_1 and k_2 are sliding mode gain. The chattering problem of sliding mode is largely caused by the discontinuous symbolic function. However, as shown in (30) and as will be shown in the experimental results (next section), STA can alleviate the chattering problem of traditional sliding mode to a great extent by adding a continuous term before the symbolic function and putting the symbolic function into the higher-order derivative. The sliding mode surface is constructed based on the output error of the reference model and the adjustable model

$$S_\mathrm{t} = \varepsilon = \left(i_d \hat{i}_q - \hat{i}_d i_q - \frac{\psi_m}{L}\left(i_q - \hat{i}_q\right) \right) \tag{31}$$

Combined with the mathematical model of PMSM, the derivative of (31) can be obtained as

$$\begin{aligned} \dot{S}_\mathrm{t} = \dot{\varepsilon} = {} & \dot{i}_d \hat{i}_q + i_d \dot{\hat{i}}_q - \dot{i}_q \hat{i}_d - i_q \dot{\hat{i}}_d - \psi_m \left(\dot{i}_q - \dot{\hat{i}}_q\right)/L = \\ & \left(\omega_\mathrm{r} - \hat{\omega}_\mathrm{r}\right)\left(i_d \hat{i}_d + i_q \hat{i}_q + \frac{\psi_m}{L}\left(i_d + \hat{i}_d\right) + \left(\frac{\psi_m}{L}\right)^2 \right) + \\ & \left(2RL\left(\hat{i}_d i_q - i_d \hat{i}_q\right) + u_q L\left(i_d - \hat{i}_d\right) + \left(R\psi_m - u_d L\right)\left(i_q - \hat{i}_q\right)\right)/L^2 \end{aligned} \tag{32}$$

It can be seen that when the system state enters the sliding mode, i.e., $S_\mathrm{t} = \dot{S}_t = 0$, the error between the output of the reference model and the adjustable model will converge to zero, and the estimated speed obtained by the observer will reach the actual value. After some further arrangement of (31) and (32), the adaptive mechanism for speed estimation based on STA can be expressed as

$$\hat{\omega}_\mathrm{r} = k_p \left| S_\mathrm{t} \right|^{0.5} \operatorname{sign}\left(S_\mathrm{t}\right) + \int_0^t k_i \operatorname{sign}\left(S_\mathrm{t}\right) \mathrm{d}t \tag{33}$$

$$\hat{\theta} = \int_0^t \hat{\omega}_\mathrm{r} \mathrm{d}t \tag{34}$$

where $\hat{\theta}$ is the estimated rotor position and the structural block diagram of STA-MRASO is shown in Fig. 3.

Fig. 3. The block diagram of STA-MRASO with error correction link.

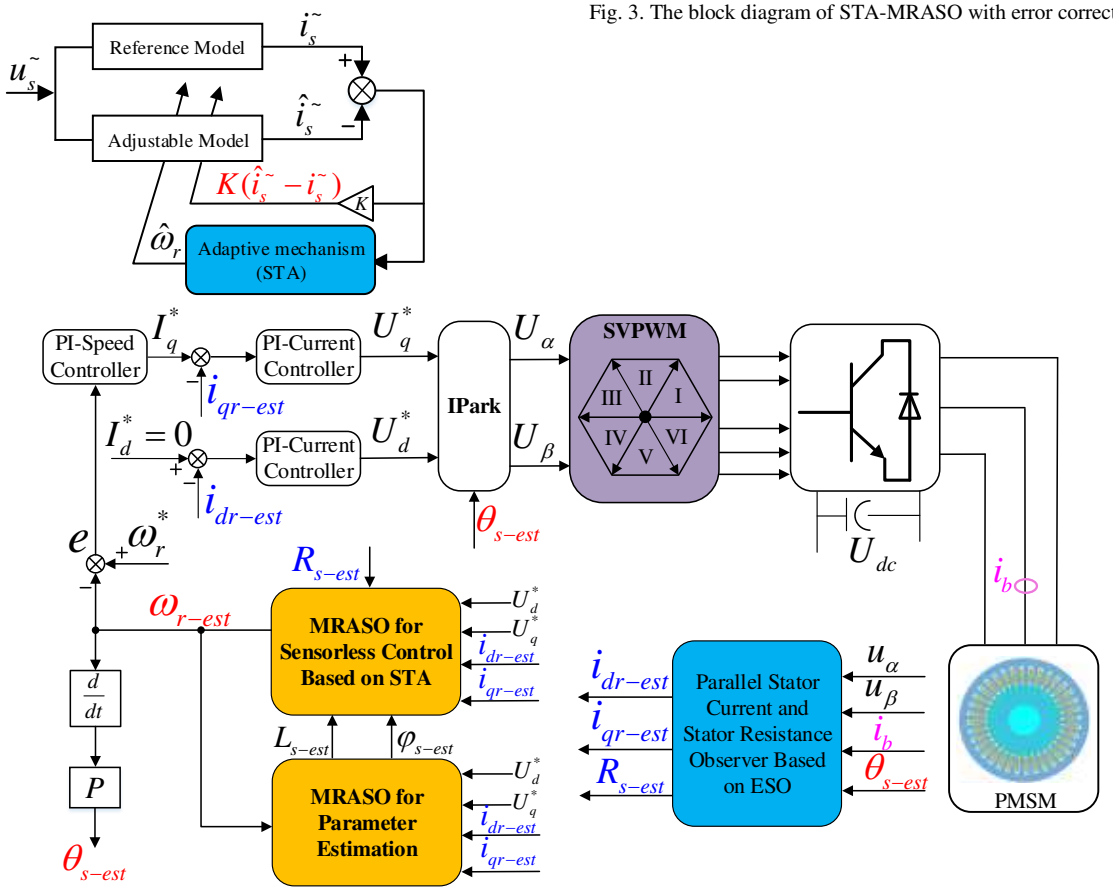

Fig. 4. The proposed SO-ESO based parallel rotor speed and multi-parameter estimation with B-phase current sensor.

B. *ESO-MRASO for Parameter Estimation*

From (35), it can be noted that the estimation of rotor speed is largely affected by the PMSM parameters (i.e., stator resistance, inductance, and flux). These parameters change with load current and motor temperature. This is why the MRASO is not robust to parameter variation. Therefore, the second MRASO only needs to identify the inductance and permanent flux parameters because the resistance is estimated by SO-ESO. The second MRASO and SO-ESO update the identified electrical parameters to the second MRASO to achieve high robust sensorless control as shown in Fig. 4.

$$\begin{pmatrix} \dot{i}_q \\ \dot{i}_d \end{pmatrix} = \begin{bmatrix} -\frac{R}{L} & -\omega_r \\ \omega_r & -\frac{R}{L} \end{bmatrix} \begin{pmatrix} i_q \\ i_d \end{pmatrix} + \begin{bmatrix} \frac{1}{L} & 0 \\ 0 & \frac{1}{L} \end{bmatrix} \begin{pmatrix} u_q \\ u_d \end{pmatrix} + \begin{bmatrix} -\frac{\psi_m}{L}\omega_r \\ 0 \end{bmatrix} \tag{35}$$

According to the above structure, three state space elements a, b, and c are introduced. Let

$$a = \frac{R}{L},\ b = \frac{1}{L},\ c = \frac{\psi_m}{L} \tag{36}$$

Introduce three coefficient matrices A, B, and C as follows

$$\frac{di}{dt} = Ai + Bu + C \tag{37}$$

where $i = \left[i_q, i_d\right]^T$, $u = \left[u_q, u_d\right]^T$ are the stator current vector and stator voltage vector, respectively. $A = \begin{pmatrix} -a & -\omega_r \\ \omega_r & -a \end{pmatrix}$, $B = \begin{pmatrix} b & 0 \\ 0 & b \end{pmatrix}$, and $C = \left[-c\omega_r \quad 0\right]^T$.

When identifying the parameters of the PMSM, it can be assumed that the value of the speed is available, so equation (37) can be expressed as an adjustable form:

$$\frac{d\hat{i}}{dt} = \hat{A}\hat{i} + \hat{B}u + \hat{C} + K\hat{i}_e \tag{38}$$

where $\hat{i} = \left[\hat{i}_q, \hat{i}_d\right]^T$, K is the gain, $\hat{A}$, $\hat{B}$ and $\hat{C}$ are the estimated values of A, B and C, respectively.

According to (37) and (38), the following equation can be obtained:

$$\frac{d(i-\hat{i})}{dt} = (Ai - \hat{A}\hat{i}) + (Bu - \hat{B}u) + (C - \hat{C}) - K\hat{i}_e \tag{39}$$

Let $H = \dfrac{d\left(i-\hat{i}\right)}{dt}$ then (39) can be expressed as

$$H = (A+K)e + \Delta A\hat{i} + \Delta Bu + \Delta C \tag{40}$$

where $e = i - \hat{i}$ is the error vector. The coefficient matrix is the expression form of each difference.

Now we adopt and apply Popov's hyperstability theory to analyze the stability of the system. In order to construct the Popov integral inequality, equation (40) is simplified as

$$H = (A+K)e + W \tag{41}$$

where $W = \Delta A\hat{i} + \Delta Bu + \Delta C$.

According to Popov stability theorem, the transfer function matrix of the system must meet the positive real condition, and

the designed parameter adaptation rate must meet the requirements of Popov integral inequality:

$$\eta(0,t_1)=\int_0^{t_1} e^T W dt \le \gamma_0^2=\int_0^{t_1} e^T(\Delta A\hat{i}+\Delta Bu+\Delta C)dt \le \gamma_0^2 \quad (42)$$

Let $I=\begin{pmatrix}1&0\\0&1\end{pmatrix}$, and then the following inequality holds

$$\int_0^{t_1}\left(\Delta Ae^T\hat{i}-\Delta Be^T Iu+\Delta Ce^T\omega_r\right)dt \ge -\gamma_0^2 \quad (43)$$

Equation (43) can be decomposed into the following parts

$$\int_0^{t_1}\Delta Ae^T I\hat{i}dt \ge -\gamma_1^2,\ \int_0^{t_1}\Delta Be^T Iudt \ge -\gamma_2^2,\ \int_0^{t_1}\Delta Ce^T\omega_r dt \ge -\gamma_3^2 \quad (44)$$

To design the parameters γ_1,γ_2 and γ_3 to be identified in the form of proportional integral, define:

$$\hat{a}=\int_0^t\Phi_a(e)d\tau+\hat{a}(0),\ \hat{b}=\int_0^t\Phi_b(e)d\tau+\hat{b}(0),\ \hat{c}=\int_0^t\Phi_c(e)d\tau+\hat{c}(0)$$

And introduce the following formula:

$$\int_0^t\frac{df(t)}{dt}f(t)dt=\int_0^t f(t)df(t)=\frac{1}{2}\left[f^2(t)-f^2(0)\right]\ge\frac{1}{2}f^2(0) \quad (45)$$

Let $\frac{df(t)}{dt}=e^T\hat{i}$ and we can obtain

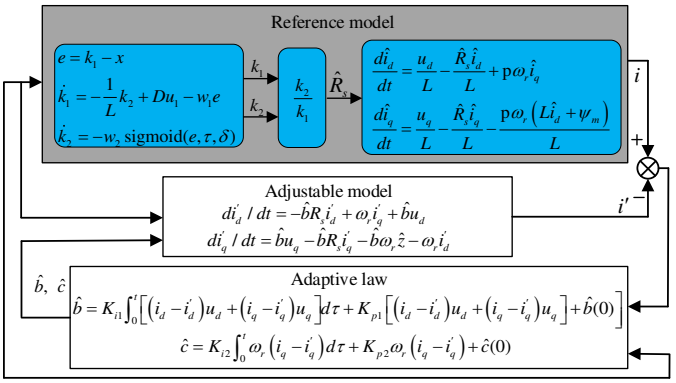

Fig. 5. The block diagram of SO-ESO based MRASO for parameter estimation with B-phase current sensor.

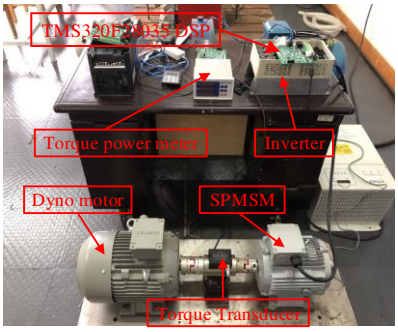

Fig. 6. The used prototype PMSM.

$$\begin{cases}\hat{a}=-\left(K_{p1}+\dfrac{K_{i1}}{s}\right)\left(\hat{i}_d e_d+\hat{i}_q e_q\right)+\hat{a}(0)\\ \hat{b}=\left(K_{p2}+\dfrac{K_{i2}}{s}\right)\left(u_d e_d+u_q e_q\right)+\hat{b}(0)\\ \hat{c}=-\left(K_{p3}+\dfrac{K_{i3}}{s}\right)w_r e_q+\hat{c}(0)\end{cases} \quad (46)$$

Note that $\hat{a}$, $\hat{b}$, and $\hat{c}$ are mathematical related to the parameters to be identified. The adaptive rates of resistance, inductance and flux can be obtained simultaneously. Also note that when only one or two parameters need to be identified, the identification accuracy can be improved. Since the stator resistance is obtained by SO-ESO, the second MRASO only needs to identify the inductance and permanent flux as shown in Fig. 5.

IV. Experimental Waveforms and Analysis

A. Configuration of the Platform

The DC bus is connected with the dc power source whose output is fixed to 311V, and the sampling frequency is set to 11.5 kHz. The TMS320F28335 DSP is employed for parameter estimation of the prototype machine. All experiments are carried out on the same computer with intel(R) core(TM) i5-7500, four-core processors, RAM 16 GB and GPU of NVIDIA GeForce GTX 1050 Ti. The design parameters are exhibited in Table I. The schematic diagrams of the hardware and software platforms are shown in Fig. 6 and 7. The relevant simulation results are exhibited to demonstrate the robustness of SO-ESO based parallel parameter estimation and sensorless control. In all the tests, the double-closed-loop system is adopted and the load torque is set to 20N.

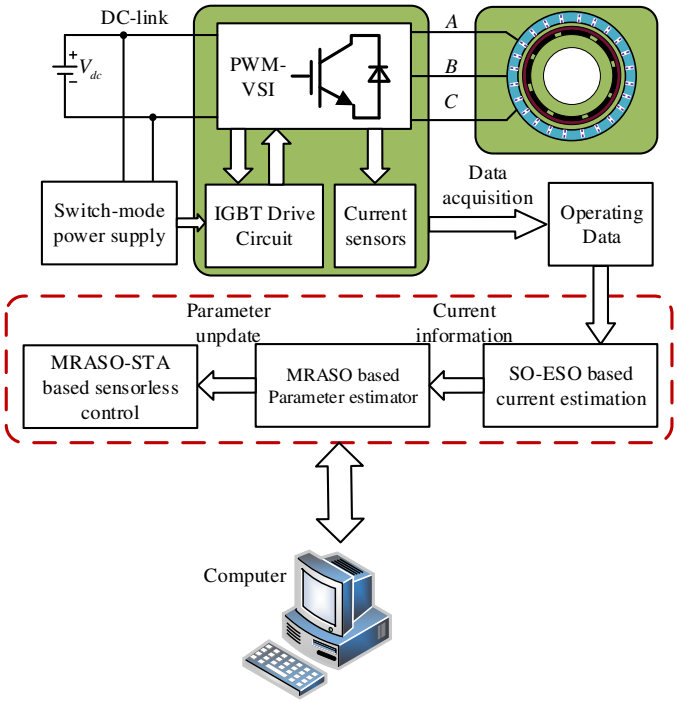

Fig. 7. The schematic structure of hardware and software platform framework.

TABLE I
Design Parameters and Specification of the PMSM

Parameters	Values	Parameters	Values
Nominal speed	3000 rpm	Stator resistance	1.204 Ω
Nominal current I_N	6.8 A	*d/q* axis inductance	15.86 mH
Nominal voltage U_N	380 V	Permanent flux	79 mWb
Nominal power	4.0 kW	Number of pole pairs	4

B. *Experimental Results and Analysis*

In order to show the superiority and robustness of the introduced sensorless control based on current estimation, the following two schemes are introduced and investigated.

The Step Change of Reference Speed: In this experiment, the speed was set to be step signal but the stator resistance remains to be 1.204Ω. The step response (10 rpm → 20 rpm → 30 rpm → 40 rpm → 50 rpm) and the estimated values of the rotor speed are exhibited in Fig. 8(a). It exhibits that the overshoot and rise time is small in the speed transition. Furthermore, the scheme based on MRASO-STA has smaller overshoot and shorter rise time. The error is large only when the speed suddenly changes such as at 1s, 2s, 3s, and 4s. Fig. 8(b) shows that the rotor position estimation error based on MRASO-STA is smaller than that of MRASO-PI. Because the speed error is large in the beginning, the estimated error of position is also large. In addition, it can be seen that the estimated *d*-axis current using SO-ESO is very close to 0 as shown in Fig. 8(c). The reference speed is set as 500 rpm → 1000 rpm → 1300 rpm → 1200rpm → 500 rpm, and these are shown in Fig. 9(a), where it can be seen that the dynamic performance is excellent based on MRASO-STA. Fig. 9(b) exhibits the corresponding rotor position estimation error and Fig. 9(c) shows the estimated *d*-axis current. Because the 'i_d = 0' control strategy is adopted, 'Ref i_d' is zeros. It can be seen that the estimated *d*-axis current is closer to zero based on MRASO-STA. It shows that the SO-ESO based sensorless control with

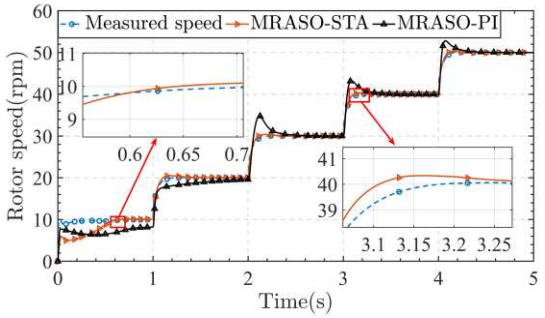

(a)

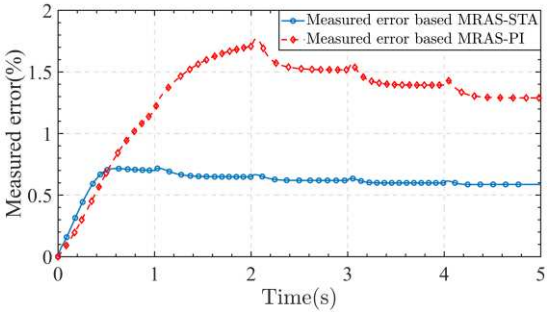

(b)

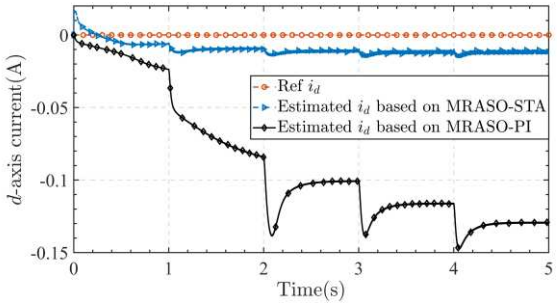

(c)

Fig. 8. The experimental results for speed estimation based on STA-MRASO at 1.204Ω. (a) Step change of reference speed (10 rpm → 20 rpm → 30 rpm → 40 rpm → 50 rpm). (b) The measured error of estimated rotor position. (c) The measured and estimated *d*-axis current wave.

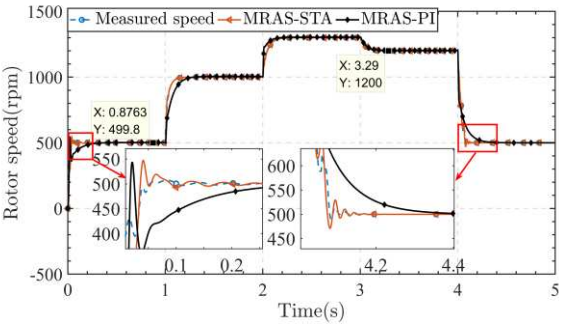

(a)

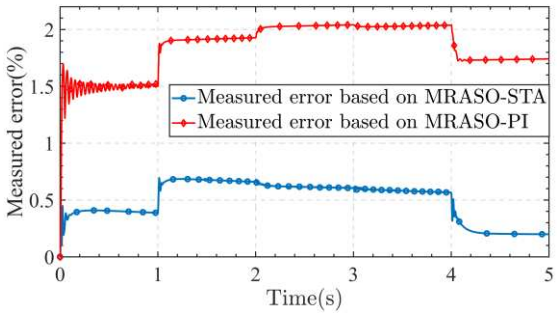

(b)

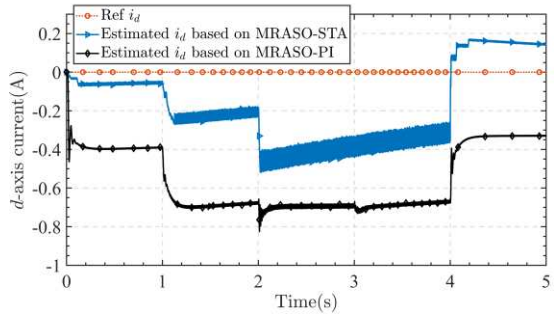

(c)

Fig. 9. The experimental results for speed estimation based on STA-MRASO at 1.204Ω. (a) Step change of reference speed (500 rpm → 1000 rpm → 1300 rpm → 1200 rpm → 500 rpm). (b) The measured error of estimated rotor position. (c) The measured and estimated *d*-axis current wave.

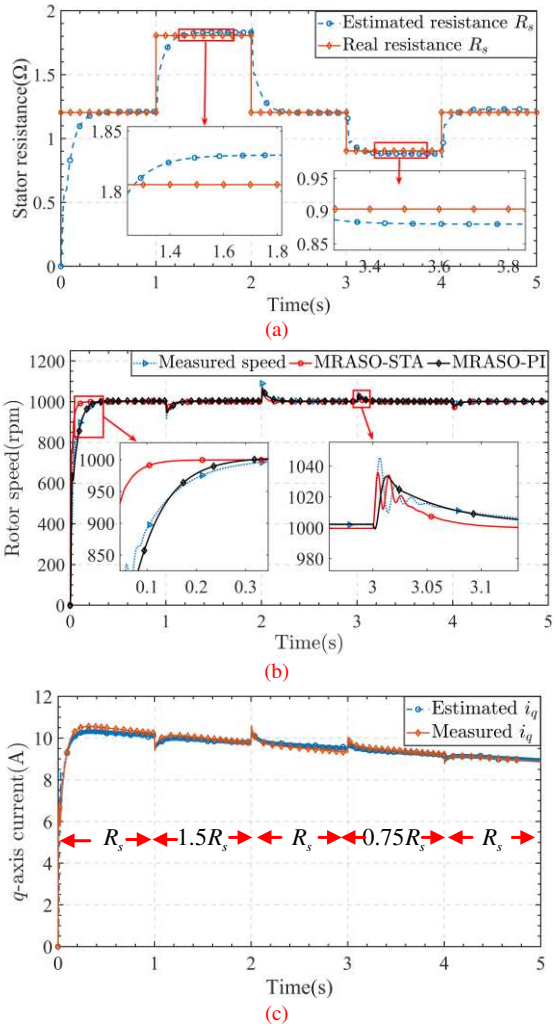

Fig. 10. The experimental results for the estimation of stator resistance and q axis current using SO-ESO under 1000rpm. (a) under resistance variation (1.204Ω → 1.806Ω → 1.204Ω → 0.903Ω → 1.204Ω). (b) Speed estimation based on STA-MRASO. (c) The measured and estimate Q-axis current wave

B-phase current sensor has an excellent control performance, and can be further improved based on MRASO-STA.

2) *The Step Change of Stator Resistance:* In practice, the resistance of PMSM usually varies with the temperature. To reflect this fact and verify the robustness of control performance, in the experiments the big change of stator resistance is considered accordingly, and the reference speed

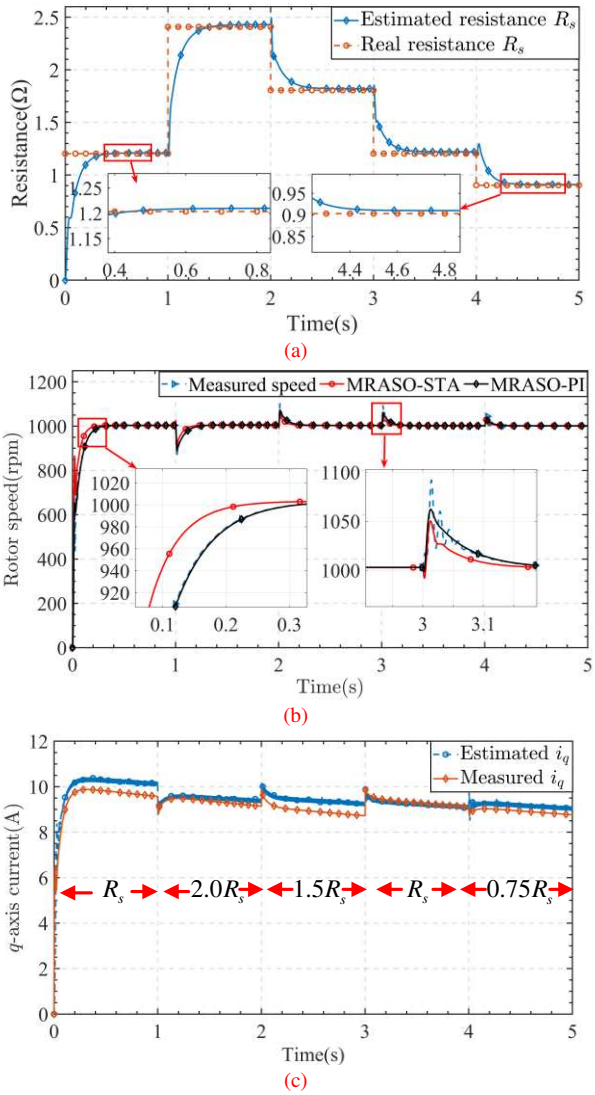

Fig. 11. The experimental results for the estimation of stator resistance and *d*/*q* axis current using SO-ESO under 1000rpm. (a) under resistance variation (1.204Ω → 2.408Ω → 1.806Ω → 1.204Ω → 0.903Ω). (b) Speed estimation based on STA-MRASO. (c) The measured and estimate *q*-axis current wave.

is set as 1000 rpm. The experimental results based on two sets of resistance changes are shown in Fig. 10 and Fig. 11, where 'Real resistance' represents the reference value of stator resistance. In Fig. 10(a), the change process of resistance is as follows: 1.204Ω (initial value) → 1.806Ω (1.5 times of the initial value) → 1.204Ω → 0.903Ω (0.75 times of the initial value) → 1.204Ω. It shows that the SO-ESO has a higher accuracy for estimating the stator resistance. Fig. 10(b) shows the relevant estimated speed when the resistance changes. It can be seen that the steady-state and dynamic performance based on MRASO-STA is better than that with MRASO-PI. When the resistance varies from 1.204Ω to 1.806Ω, the speed oscillates at the time of 1s and only takes 0.1 seconds to recover. Similarly, the speed changes at the time of 2s, 3s, and 4s due to the changes of the resistance. The waveforms of *q* axis current are shown in Fig. 10(c) and the estimated *q*-axis current is very close to the actual current, showing that the method can accurately estimate the actual current without current sensor. In Fig. 11(a), the change process of resistance is as follows: 1.204Ω

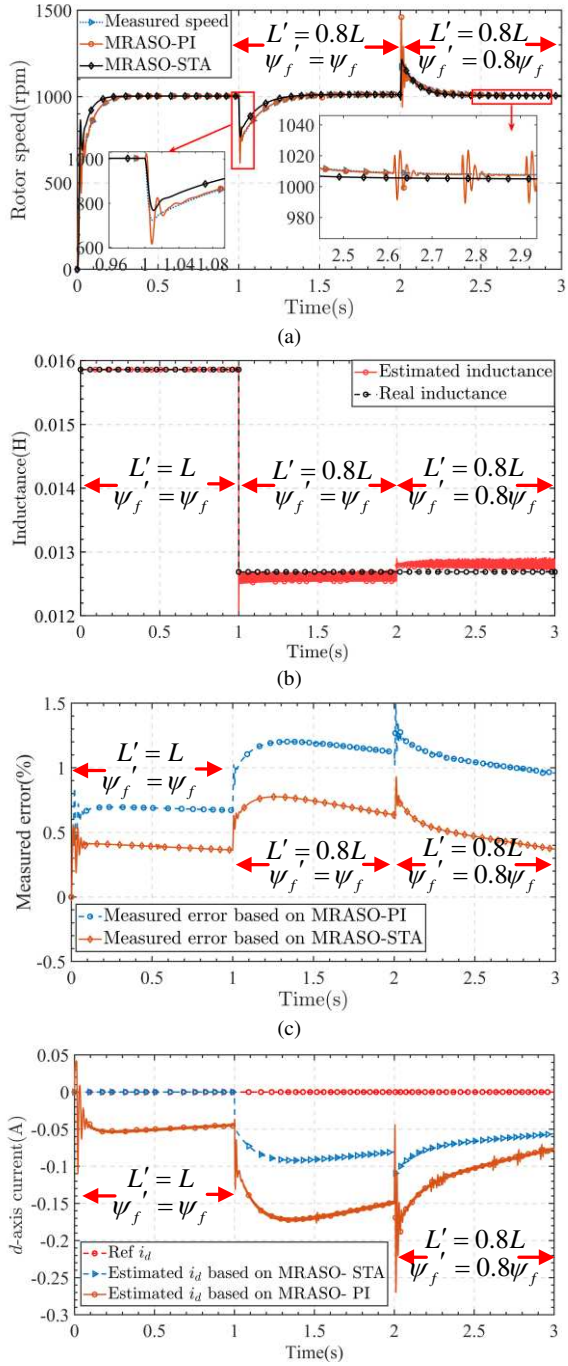

Fig. 12. The experimental results for parameter estimation at 1.204Ω under 1000rpm. (a) Speed estimation based on STA-MRASO. (b) The estimation of inductance. (c) The measured error of estimated rotor position. (d) The measured and estimated *d*-axis current wave.

(initial value) → 2.408Ω (2.0 times of the initial value) → 1.806Ω (1.5 times of the initial value) → 1.204Ω →0.903Ω (0.75 times of the initial value). It shows that the steady-state error is less than 5.2%. Since the real resistance is doubled at 1s, the response of speed drop is larger than Fig. 10(b) but it returns to stability immediately as shown in Fig. 11(b). Fig. 11(c) exhibits the corresponding *q* axis current. It shows good robustness to the sudden change of stator resistance.

3) *The Step Change of permanent flux and inductance:* In addition to the sudden change of stator resistance, PMSM

may have a demagnetization fault, resulting in the reduction of flux linkage. Therefore, the flux linkage step change needs to be taken into account. The inductance does not change during the flux linkage mutation process. Fig. 12 shows the scenario where the inductance reduces to 80% of its initial value at t =1 s, while the permanent magnet flux chain reduces to 80% its initial value at t = 2 s. The real value of inductance is 15.86mH. Due to the sudden change in inductance and flux linkage, the speed vibrates for a short period and then returns to the initial value, as shown in Fig. 12(a). Furthermore, the speed estimation based on MRASO-STA scheme is more robust to parameter perturbation compared with MRASO-PI. It can be seen from Fig. 12(b) that high-precision parameter identification can be achieved based on the second MRASO, and the sudden change in permanent magnet flux linkage will have little effect on inductance identification at the second jump (t = 2 s). As can be seen from Fig. 12(c) and (d), MRASO-STA has better dynamic performance and steady-state performance under parameter perturbation than MRASO-PI. Therefore, the performance of the muti-parameter estimation for PMSM is effective in the proposed MRASO.

V. Conclusion

In this paper, a SO-ESO based parallel rotor speed and multi-parameter estimation method with B-phase current sensor is introduced for PMSM, which can reduce the overshoot of stator resistance tracking and enhance the reliability of sensorless control. Experiments under variable speed and variable electrical parameters have been carried out. The following results have been obtained:

1) The introduced SO-ESO can accurately estimate the *d*/*q* axis current with a small steady-state error. In addition, the MRASO-STA with error correction term can obtain better dynamic performance and has a strong robustness to parameter variation compared to the traditional MRASO-PI.

2) When the stator resistance changes from a range between of 0.9 to 2.0 times of an initial value, the SO-ESO can track closely and the estimation error is less than 4.8%. In addition, the overshoot of the estimated stator resistance is small even if there is a sudden change.

3) Even when the inductance reduces to 80% of its initial value, it can still be accurately identified. Furthermore, the inductance and permanent magnet flux are identified and then iterated into the MRASO-STA to update the parameters in real time, so that strong robustness control for the motor can be achieved when parameters change.

In conclusion, with the proposed scheme, the performance of PMSM sensorless control is more robust and reliable. In future, more experiments will be performed on an actual platform to further test the performance of the proposed control scheme and extend its applications.

References

[1] F. Bu et al., "Rotor Position Tracking Control for Low Speed Operation of Direct-Drive PMSM Servo System," *IEEE/ASME Trans. Mechatron*., vol. 26, no. 2, pp. 1129-1139, April 2021.

[2] X. Zhou, S. Li, M. Lu, F. Zeng, M. Zhu and Y. Yu, "New Fault Tolerance Method for Open-Phase PMSM," *IEEE Access*, vol. 7, pp. 146416-146427, 2019.

[3] X. Sun, Z. Shi, G. Lei, Y. Guo and J. Zhu, "Analysis and Design Optimization of a Permanent Magnet Synchronous Motor for a Campus Patrol Electric Vehicle," *IEEE Trans. Veh. Tech*., vol. 68, no. 11, pp. 10535-10544, Nov. 2019.

[4] S. Li, S. Zheng, X. Zhou and J. Fang, "A Novel Initial Rotor Position Estimation Method at Standstill for Doubly Salient Permanent Magnet Motor," *IEEE Trans. Ind. Inform*., vol. 14, no. 7, pp. 2914-2924, July 2018.

[5] Q. Teng, H. Cui, J. Duan, J. Zhu, Y. Guo and G. Lei, "Extended state observer-based vector control for PMSM drive system with single phase current sensor," in *2017 20th International Conference on Electrical Machines and Systems (ICEMS)*, 2017, pp. 1-6.

[6] A. V. R. Teja, V. Verma, and C. Chakraborty. "A New Formulation of Reactive-Power-Based Model Reference Adaptive System for Sensorless Induction Motor Drive," *IEEE Trans. Ind. Electron*., vol. 62, no. 11, pp. 6797-6808, Nov. 2015.

[7] Y. M. Zhang and J. Jiang. "Bibliographical review on reconfigurable fault-tolerant control systems," Annual Reviews in Control, vol. 32, no. 2, pp. 229–252, 2008.

[8] X. Wang, Z. Wang, Z. Xu, M. Cheng, W. Wang, and Y. Hu, "Comprehensive Diagnosis and Tolerance Strategies for Electrical Faults and Sensor Faults in Dual Three-Phase PMSM Drives," *IEEE Trans. Power Electron.*, vol. 34, no. 7, pp. 6669-6684, 2019.

[9] J. T. Boys. "Novel current sensor for PWM ac drives," *IEE Proceedings: Electric Power Applications*, vol. 135, pp. 27-32, 1988.

[10] H. Y. Ma, K. Sun, Q. Wei, et al. "Phase current reconstruction for AC motor adjustable speed drives in the over modulation method," *Journal of Tsinghua University*, vol. 50, no. 11, pp. 1757-1761, 2010.

[11] H. Lu, X. Cheng, W. Qu, et al. "A 3-phase Current Reconstruction Technique Using Single DC Current Sensor Based on TSPWM," *IEEE Trans. Power Electron.*, vol. 29, no. 3, pp. 1542-1550, 2014.

[12] S. C. Yang. "Saliency-based position estimation of permanent-magnet synchronous machines using square wave voltage injection with a single current sensor," *IEEE Trans. Ind. Appl.*, vol. 51, no. 2, pp. 1561-1571, 2015.

[13] Y.X. Xu, H. Yan, J.B. Zou, et al. "Zero Voltage Vector Sampling Method for PMSM 3-phase Current Reconstruction Using Single Current Sensor," *IEEE Trans. Power Electron*.,vol. 32,no. 5, pp. 3797-3807, 2016.

[14] Q. F. Teng, J. Y. Bai, J. G. Zhu, et al. "Current sensorless model predictive torque control based on adaptive backstepping observer for PMSM drives," WSEAS Transactions on systems, vol. 13, pp. 187-202, 2014.

[15] C. M. Verrelli et al., "Speed Sensor Fault Tolerant PMSM Machines: From Position-Sensorless to Sensorless Control," *IEEE Trans. Ind. Appl*, vol. 55, no. 4, pp. 3946-3954, Jul.-Aug. 2019.

[16] H. Nian and W. Hu, "A Sensorless Drive Strategy for Open-End Winding PMSM With Common DC Voltage Based on Lower Switching Frequency," *IEEE Trans. Energy Convers*., vol. 34, no. 3, pp. 1553-1562, Sept. 2019.

[17] T. Wang et al., "An EMF Observer for PMSM Sensorless Drives Adaptive to Stator Resistance and Rotor Flux Linkage," *IEEE J. Emerg. Sel. Topics Power Electron*., vol. 7, no. 3, pp. 1899-1913, Sept. 2019.

[18] X. Luo, A. Shen, Q. Tang, J. Liu and J. Xu, "Two-Step Continuous-Control Set Model Predictive Current Control Strategy for SPMSM Sensorless Drives," *IEEE Trans. Energy Convers*., vol. 36, no. 2, pp. 1110-1120, June 2021.

[19] K.-B. Lee and F. Blaabjerg, "Reduced-order extended Luenberger observer based sensorless vector control driven by matrix converter with nonlinearity compensation," *IEEE Trans. Ind. Electron*., vol. 53, no. 1, pp. 66–75, Feb. 2005.

[20] P. Liu, C.-Y. Hung, C.-S. Chiu, and K.-Y. Lian, "Sensorless linear induction motor speed tracking using fuzzy observers," *IET Electr. Power Applicat*., vol. 5, no. 4, pp. 325–334, Apr. 2011.

[21] M. Cuibus, V. Bostan, S. Ambrosii, C. Ilas, and R. Magureanu, "Luenberger, Kalman and neural network observers for sensorless induction motor control," in *Proc. 3rd Int. Power Electron. Motion Control Conf*., 2000, vol. 3, pp. 1256–1261.

[22] E. Zerdali and M. Barut, "MRAS based real-time speed-sensorless control of induction motor with optimized fuzzy-PI controller," in *Proc. 2013 IEEE International Symposium on Sensorless Control for Electrical Drives and Predictive Control of Electrical Drives and Power Electronics (SLED/PRECEDE),* Munich, pp. 1-5, 2013.

[23] S. E. Rezgui, S. Legrioui, A. Mehdi, and H. Benalla, "Robust IM control with MRAS-based speed and parameters estimation with ANN

using exponential reaching law," in *Proc. 2014 International Conference on Control, Decision and Information Technologies (CoDIT)*, Metz, pp. 477-482, 2014.

[24] S. E. Rezgui, S. Legrioui, A. Mehdi and H. Benalla, "Robust IM control with MRAS-based speed and parameters estimation with ANN using exponential reaching law," *2014 International Conference on Control, Decision and Information Technologies (CoDIT)*, Metz, 2014, pp. 477-482.

[25] Y. B. Zbede, S. M. Gadoue and D. J. Atkinson, "Model Predictive MRAS Estimator for Sensorless Induction Motor Drives," *IEEE Trans. Ind. Electron*., vol. 63, no. 6, pp. 3511-3521, June 2016.

[26] S. A. Davari, F. Wang and R. M. Kennel, "Robust Deadbeat Control of an Induction Motor by Stable MRAS Speed and Stator Estimation," *IEEE Trans. Ind. Inform*., vol. 14, no. 1, pp. 200-209, Jan. 2018.

[27] T. Zwerger and P. Mercorelli, "Combining SMC and MTPA Using an EKF to Estimate Parameters and States of an Interior PMSM," *2019 20th International Carpathian Control Conference (ICCC)*, 2019, pp. 1-6.

[28] O. C. Kivanc and S. B. Ozturk, "Sensorless PMSM Drive Based on Stator Feedforward Voltage Estimation Improved With MRAS Multiparameter Estimation," *IEEE/ASME Trans. Mechatron*., vol. 23, no. 3, pp. 1326-1337, June 2018.

[29] H. Lu, S. Yang, M. Zhao and S. Cheng, "Multi-Robot Indoor Environment Map Building Based on Multi-Stage Optimization Method," *Complex System Modeling and Simulation*, vol. 1, no. 2, pp. 145-161, June 2021.

[30] H. Yang, R. Yang, W. Hu and Z. Huang, "FPGA-Based Sensorless Speed Control of PMSM Using Enhanced Performance Controller Based on the Reduced-Order EKF," *IEEE J. Emerg. Sel. Topics Power Electron*., vol. 9, no. 1, pp. 289-301, Feb. 2021.

[31] A. Balamurali, C. Lai, G. Feng, V. Loukanov, and N. C. Kar, "Online multi-parameter identification of permanent magnet synchronous motors in EV application considering iron losses," in *Proc. 2016 XXII International Conference on Electrical Machines (ICEM)*, Lausanne, pp. 2306-2312, 2016.

[32] Z. Li, G. Feng, C. Lai, D. Banerjee, W. Li and N. C. Kar, "Current Injection-Based Multi-parameter Estimation for Dual Three-Phase IPMSM Considering VSI Nonlinearity," *IEEE Trans. Transport. Electrific*., vol. 5, no. 2, pp. 405-415, June 2019.

[33] Z. -H. Liu, J. Nie, H. -L. Wei, L. Chen, X. -H. Li and H. -Q. Zhang, "A Newly Designed VSC-Based Current Regulator for Sensorless Control of PMSM Considering VSI Nonlinearity," *IEEE J. Emerg. Sel. Topics Power Electron*., vol. 9, no. 4, pp. 4420-4431, Aug. 2021.

[34] K.-H. Kim, "DSP-based sequential parameter estimation of PWM inverter fed IPM synchronous machine for auto-tuning applications," *Int. J. Control Autom*., vol. 6, no. 2, pp. 195–204, Apr. 2013.

[35] C. Zhou et al., "An Improved Direct Adaptive Fuzzy Controller of an Uncertain PMSM for Web-Based E-Service Systems," *IEEE Trans. Fuzzy Syst.*, vol. 23, no. 1, pp. 58-71, Feb. 2015.

[36] R. Krishnan. "Permanent Magnet Synchronous and Brushless DC Motor Drives," *CRC Press/Taylor & Francis*, 2017.